REPORT DOCUMENTATION PAGE

Form Approved
OMB No. 0704-0188

1. AGENCY USE ONLY (Leave blank)	2. REPORT DATE	3. REPORT TYPE AND DATES COVERED
	1995	Interim

4. TITLE AND SUBTITLE

The Interplay Between Geometric and Electronic Structure and the Magnetism of Small Pd Clusters

5. FUNDING NUMBERS

N00014-90-J-1608
G

6. AUTHOR(S)

Guillermina Lucia Estiu and Michael C. Zerner

7. PERFORMING ORGANIZATION NAME(S) AND ADDRESS(ES)

University of Florida
Department of Chemistry
Gainesville, FL 32611 USA

8. PERFORMING ORGANIZATION REPORT NUMBER

9. SPONSORING/MONITORING AGENCY NAME(S) AND ADDRESS(ES)

Office of Naval Research
Chemistry Division Code 1113
Arlington, VA 22217-5000

10. SPONSORING/MONITORING AGENCY REPORT NUMBER

Technical Report 36

11. SUPPLEMENTARY NOTES

[redacted]

12a. DISTRIBUTION/AVAILABILITY STATEMENT

This document has been approved for public release: its distribution is unlimited.

12b. DISTRIBUTION CODE

13. ABSTRACT (Maximum 200 words)

See attached Abstract.

14. SUBJECT TERMS	15. NUMBER OF PAGES: 28
	16. PRICE CODE

17. SECURITY CLASSIFICATION OF REPORT	18. SECURITY CLASSIFICATION OF THIS PAGE	19. SECURITY CLASSIFICATION OF ABSTRACT	20. LIMITATION OF ABSTRACT
Unclassified	Unclassified	Unclassified	SAR

THE INTERPLAY BETWEEN GEOMETRIC AND ELECTRONIC STRUCTURE AND THE MAGNETISM OF SMALL Pd CLUSTERS

Guillermina Lucía Estiú
Programa Quinor. Facultad de Ciencias Exactas.
Universidad Nacional de La Plata. Casilla de Correo 962
-1900- La Plata, ARGENTINA.

Michael C. Zerner
Quantum Theory Project, Department of Chemistry and
Physics, University of Florida.
Gainesville, Florida 32611 -USA-

Rec Dec 1, 1993

- ABSTRACT -

The electronic structure and geometric characteristics of small Pd clusters (up to 13 atoms) are studied at the SCF/CI level, with major focus on the mutual dependence between these properties. To this end, Jahn-Teller effects have been considered, and the magnetic moments analyzed on the distorted, most stable, structures.

By means of calculations of the INDO type, the energies and normal modes involved in the different steps of the distortions which leads to diamagnetic Pd_{13} but paramagnetic Pd_4 are described. Comparisons with other calculations and experimental data are included.

1- INTRODUCTION -

The potential uses of metal clusters in chemistry, physics and technology have lead to impressive effort towards a better understanding of their properties. Because their characterization represents an important link in the understanding of the fundamental mechanisms of catalysis, the basic properties (geometry, bond strength, reactivity) of small metal aggregates have become the subject of intense theoretical [1-13] and experimental study [14-21].

It is well known that the electronic properties and structural characteristics of metal aggregates are different from the bulk [20-22]. The nature of these differing electronic properties is believed to play an important role in the adsorption and reaction of small molecules, and is largely related to geometry [6,16,23,24]. Metal clusters of suitable size are able to reproduce the electronic features of crystal defects and of the small metal particles in supported structures that are responsible for catalytic reactivity.

Research on the electronic structure and geometry of small metal clusters may lead to the development of more selective and efficient catalysts, and to model specific reactions through the analysis of the interactions involved in the adsorption of simple molecules.

As the simplest representation of the reactive site, often metal clusters defined by 2 to 100 atoms are studied, with particular emphasis in the change of the properties as a function of the size [3,4,6,10]. However, as has been previously described, not only the size, but also the geometric and electronic structure are important to reproduce *surface defects* or *metal particles* in supported catalysts. Besides, the experimental information available on the geometrical structure of metallic clusters of the order of 10 atoms is indirect [15,20,21] and, in most cases,not even the symmetries are known. Any calculation of the physical properties of microclusters has to start, therefore, by the prediction of the geometry by means of the minimization of the total energy. On the other hand, the most symmetrical configurations of small clusters are very often

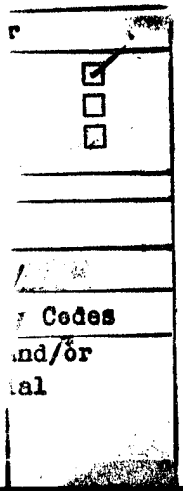

A-1

unstable due to the Jahn-Teller effect [1,4,7,25]. The calculations that only consider highly symmetric geometries often miss the true equilibrium geometry. For a detailed understanding of the structure-reactivity relationships in clusters, and a successful correlation between chemical and physical properties, the most stable structure of the cluster must first be determined. However, because of the unquestionable coupling between electronic and geometric structure, clearly shown by the importance of the Jahn-Teller distortions [7], both are to be determined simultaneously when an interpretation of the reactivity is the goal.

This mutual dependence follows from the consideration of two coupled effects:

The non-equivalent occupation of energetically degenerate orbitals leads to a splitting of the degeneracy, by means of a distortion of the geometry to a lower symmetry one. The structure of the cluster is determined by Jahn-Teller effects.

Elemental clusters, on the other hand, have the tendency to assume highly symmetric structures, as a consequence of which degeneracy in the one-electron levels occur (effect of the geometry on the electronic structure). Only those systems with a number of electrons sufficient to completely fill or half-fill the sets of degenerate one- electron levels will not Jahn-Teller distort.

This electronic structure- geometry interplay opens a challenging field in the study of the characteristics of metal clusters, when properties relevant to catalysis (local density charges, magnetic moments) are to be analyzed.

With the aim of better understanding the coupling between the electronic configuration and the geometry of the transition metal structures, we discuss, in this paper, the electronic and geometric characteristics of Pd clusters, evaluated at the *Self Consistent Field - Configuration Interaction* (SCF/CI) level, in an attempt to compare them with those previously found for Rh [23-25].

Different cluster sizes can be analyzed for a given transition metal. On the basis of previous results on Rh clusters [24], we have chosen a 13 atom cluster because it is large enough to provide a good description of the behavior of the tiny particles that are present in supported catalysts and small enough, on the other hand, to allow accurate calculations. A 13 atom cluster is also compatible with the representation of structures of different possible symmetries [5,25], and 13 is one of the magic numbers of atoms frequently observed in clusters of various kinds [5,26,18,19]. In addition, going from the bulk to the smaller crystallites, the density of states of transition metal 13 atom clusters [27] has been found to be close to that of the bulk. Finally we remark that often properties that bear no resemblance to the crystalline state are more frequently found: the most attractive include the larger stability of the five fold symmetry structures and the unusual magnetic properties of these systems.

From many experimental [18,19,27,28] and theoretical [3-7,10,11] investigations, it was concluded that five fold symmetry is the natural choice of small microclusters of materials that crystalize in fcc lattices. Such structures are based on a centered 13-atom icosahedron, representing the minimum energy packing configuration in mono- and bimetallic clusters [29-33]. The planes of 13 as well as 55-atom icosahedral structures resemble close packed (111) planes, the most compact and most stable single crystal structures of fcc lattices. While there is evidence that a 55 atom icosahedron likely represents the actual particle size in supported clusters, a 13 atom icosahedon is an obvious simpler target that keeps the same local properties on the reactive centers because of the identical local environment on each of the sites. This provides an extra justification for the choice of this cluster size in our studies.

According to the previous discussion we apply, in this work, a version of the Intermediate Neglect of Differential Overlap (INDO) model [34,35] at the Self Consistent Field- Configuration Interaction (SCF-CI) level, to study the results of the geometry-electronic structure coupling on the magnetic and structural

characteristics of Pd_{13} clusters. Results on Pd_4 and on the dimer Pd_2 are also reported for comparison and calibration.

2- COMPUTATIONAL DETAILS -

Because of the $4d^{10}$ ($^1S_0$) ground state of the Pd atom, open- and closed-shell electronic configurations are compatible with both an odd or an even number atom cluster. The stability of the different multiplicities (M) for a given cluster size has been compared after a complete search for the structure of minimum energy on the potential energy surface, starting from different initial geometries which are associated with the different symmetries compatible with the number of atoms that define the cluster.

The calculated geometries are the result of a full optimization of the coordinates (interatomic distances and angles), without any constraint on their variation. Optimization is based on a minimization of the gradient [36,37], evaluated analytically, using the BFGS algorithm to update the inverse Hessian matrix in successive geometry cycles. Calculations have been made at the Restricted Hartree Fock (RHF) and Restricted Open-Shell Hartree Fock (ROHF) level. Dealing with structures of high symmetry and a large number of electrons, changes in the one-electron distribution during the SCF cycles may lead to a non-equivalent occupation of degenerate orbitals which, by breaking the symmetry in the electronic distribution may result in *spurious Jahn Teller distortions*. In order to avoid this effect, we start the calculations using Configuration-Average Hartree Fock (CAHF) theory [38], with an average M for the number of electrons considered. The final geometries depend somewhat on the number of open-shell orbitals and electrons. This number has been chosen to be compatible with the size of the open-shell for the different average M (i.e., 4 electrons in 3 orbitals for M=3, but in 6 orbitals for M=6). For each of the different geometries that result from the different definition of the open-shell, the M has been chosen after CI calculations, using the orbitals of the CAHF calculation as the reference for a Rumer CI projection over pure spin states [39]. In this way, M and geometry are

simultaneously optimized, avoiding the possibility of getting trapped in spurious local minima corresponding to a stable geometry for a given electronic configuration.

For the 13 atom Pd cluster, the stability of icosahedral (I_h) precrystalline structures has been compared to that of fcc (O_h) and hcp pieces of bulk. In order to keep the I_h symmetry, it was neccessary to start with an average of 130 electrons in 78 orbitals, then decreasing the orbital space to 66 using the previous set of eigenvectors as an initial guess. These vectors then serve as starting orbitals for a calculation with 4 electrons in 3 orbitals. With a similar strategy, 130 electrons were averaged in 78 orbitals to start the SCF calculations for fcc (Oh) and hcp symmetries. The resulting orbitals were used for an intermediate calculation, before the final RHF, with 130 electrons in 65 orbitals.

In the case of Rh_4, geometry optimizations have been done for closed-shell and an average of 4 electrons in 3 orbitals, 4 electrons in 6 orbitals, and 10 electrons in 9 orbitals, corresponding, in this way, modelling possible multiplicities (M) as high as 3, 5 or 7, respectively. With this strategy, distortions in the geometry during the SCF cycles are avoided, and geometries optimized for different electronic configurations are compared after a CI that uses the resulting orbitals that mantain full symmetry.

It is clear from this work and our previous work, that correlation energy must be included in the comparison of the energies of the different geometries for a given cluster size. Final energies, as well as electronic parameters and molecular orbital interactions, are the result of multi-reference configuration interaction calculations using single excitations, MRCIS.

Two parametrizations of the INDO theory have been used in these studies: one for geometry, which utilizes two-center two-electron integrals that are calculated ab-initio; and one to calculate the electronic descriptors and compare different M at fixed geometries, that obtain these integrals empirically from atomic spectroscopy [35, 40-42]. This latter method is

parametrized directly on molecular spectroscopy at the CI singles (CIS) level, which explains our use of MRCIS for these clusters. The resonance integrals β are chosen according to formulae that takes into account different electronegativities [23], and reproduces the available experimental geometries and spectroscopy for the dimer.

More details on the method are given elsewhere [24,41].

3- RESULTS AND DISCUSSION -

3.1- Pd_2 dimer -

The ground state of transition metal dimers is often controversial, because both the symmetry and the geometry are largely dependent on the level of correlation used in the calculations.

Our MRCIS-INDO calculations give a triplet ($^3\Sigma_u^+$) ground state for Pd_2, with a leading configuration $\sigma_g^2\pi_u^4\delta_g^4\delta_u^4\pi_g^4\sigma_u^1\sigma_g^1$, and an interatomic distance of 2.46 A. The lowest exited state is a singlet ($^1\Sigma_g^+$), 0.16 eV higher in energy than the first triplet, with a Pd-Pd bond length of 2.67 A. The next triplet, $^3\Pi_g$, lies 0.44 eV above the ground state.

The Mulliken population analysis ($5s^{0.06}5p^{0.05}4d^{9.89}$ in the first exited singlet, $5s^{0.51}5p^{0.05}4d^{9.44}$ in the triplet ground state) indicates a larger contribution of the 5s orbital to the stabilization of the metal-metal bond in the triplet, shortening the bond length relative to the singlet. The $4d^{10}$ Pd atoms undergo rehybridization of orbitals in order to form the 5s bonding combination σ_g that defines the HOMO.

Our results on the spectroscopy and the geometry of the dimer are in agreement with Density Functional [43,44] and MCSCF/MRCISD calculations [45,46]. The latter has demonstrated to give results that agree well with experiment, not only for the dimer Pd_2 [45] but also for the dimer Pd_3 [46]. There is general agreement among the different authors in the well studied case of Pd_2, in contrast to the situation for Rh_2 [23]. While a mixture of configurations characterize the electronic states in Rh_2 [23,47,48], we have found that nearly pure configurations characterize the lowest lying states of Pd_2. There is also

agreement in the larger bond length in Pd_2 than in Rh_2 (2.28 A [23]), associated with a more efficient 5s-5s bonding in the latter, where no promotion energy is needed for the 5s contribution to the σ bond.

3.2- Pd_4 structures -

Four atom clusters are most frequently studied in tetrahedral symmetry as models for a (111) structure [44]. They are usually the most stable geometries for fcc habits, with a large coordination number, compatible with the directionality of the d orbitals. We have compared tetrahedral and square planar structures, and found the former 1.77 eV more stable than the latter.

The final geometry of the tetrahedral Pd_4 is strongly dependent on the number of open-shells included in the configuration average, as shown in table 1, and this is to be expected. The more states that we include in an average involving frontier orbitals and electrons, the more likely we are to include high energy states in the average. At the SCF level, RHF calculations are based on a $4d^{10}$ configuration of the atoms and lead to longer interatomic distances than the ROHF procedure. These calculations imply, through the definition of the open-shells, that the participation of the 5s orbitals is important in the stabilization of the bond. Different M have been compared at the MRCIS level for each of the structures in table 1. Independent of the specific model and the geometry, the triplet is always the most stable state.

In table 1 the geometry of the triplet is determined from the indicated calculation using the INDO/1 model with parameters determined for geometry as described in the Computational Details section. The relative energies at fixed geometry are then determined via MRCIS INDO/S calculations. For this reason energies between rows cannot be compared.

The Mulliken populations, reported for the triplets, show the larger contribution of the s orbitals to the shorter bonds. The s participation is, in turn, dependent on the open-shell definition of the initial configuration.

Lower energies are always found for an average of 4 electrons in 3 orbitals. For this definition of the open- shell, several interatomic distances, which may either result from geometry optimizations from different initial guesses or single point calculations, have been compared. As one of the single points, the interatomic distance characteristic of the bulk (2.75 A [49]) has been analyzed. The results for the different M are reported in table 1. These calculations indicate a very flat potential for Pd_4. Within the accuracy of our treatment, however, no change in the interatomic distance with the change in M can be assessed.

The most stable structure (ground state-GS) corresponds to a triplet $^3T_2$ (Fig 1), with a leading configuration $1a_1^2 1t_2^6 1e^4 1t_1^6 2e^4 2t_1^6\ 2t_2^6 2a_1^2 3t_2^4 3t_1^0$. At this geometry the singlet $^1A_1$ lies 0.40 eV higher in energy and has the same electronic assignment as the GS.

The Mulliken population analysis shows a smaller population of the s orbital in the configuration that results from RHF calculations and this leads, in turn, to longer Pd-Pd interatomic distances.

Similar calculations for the square planar geometry yield a $^3B_{1g}$ GS, with an interatomic distance of 2.34 A.
This state is 0.14 eV lower in energy than the first exited state we calculate for this structure, which is of $^1A_{1g}$ symmetry.

3.3- Pd_{13} structures -

After a full optimization of the geometry in the way previously described, the I_h symmetry is calculated to be most stable, table 2. The interatomic distance of 2.63 A among the peripheral *surface atoms* (Fig. 2) represents a compromise between the value in the diatomics (2.46 A [48]), and that in the bulk (2.75 A [49]).

The results of MRCIS calculations show that the GS is a triplet, $^3T_{2g}$ (Fig. 3), 0.21 eV lower in energy than the first exited singlet ^1H_g. These two states arise mostly from the configuration shown in Fig. 3. The next triplet, ^3G_g, is 0.28 eV above the GS, followed by two singlets, ^1G_g and ^1A_g, 0.08 and

0.25 eV higher in energy respectively . The singlet ^1A_g also arises from the configuration shown in Fig. 3. The lowest quintet ^5T_u, lies 0.73 eV above the GS (table 2). About 38 terms lie within 1.0 eV of the lowest calculated $^3T_{2g}$.

The most stable structures in either O_h or D_{3h} symmetries belong to closed-shell configurations ^1A_g and $^1A_1"$, respectively, and are about 1.7 eV less stable than the $^3T_{2g}$ GS of I_h symmetry (table 2). The triplet $^3T_{2g}$ in O_h symmetry is 0.37 eV higher in energy than the singlet ^1A_g, and the quintet of $^5T_{1u}$ symmetry is 1.15 eV higher in energy. In the hcp (D_{3h}) structure, the triplet $^3A_1"$ and the singlet $^1A_1"$ are almost degenerate, with the singlet 0.06 eV lower. The lowest quintet of $^5A_1'$symmetry is calculated to lie 1.036 eV above the GS.

We have checked the ^1A_g of O_h symmetry and the $^1A_1"$ of D_{3h} symmetry and both are true minimum on the potential energy surface.

The larger stability of five fold symmetries in small transition metal clusters has been both experimentally determined [15,20,21] and theoretically derived [5,7,11,24,50]. It is known from experiment that five fold symmetry characterizes small Co, Cu, Ni and Mg clusters [15,20,21]. Calculations are more frequently found for the lighter elements, although molecular dynamics and density functional theory, applied to Ni_{13} and Cu_{13} respectively [3,5,11], also favor the I_h symmetry. In recent density functional calculations (LSD), Reddy, Khanna and Dunlap [50] find I_h structures more stable than O_h for Pd_{13}, Rh_{13} and Ru_{13}, in agreement with our present results on Pd and those previously published for Rh [25]. However, they have not considered any decrease in the symmetry, and the large magnetic moment of the I_h clusters, which results from the partial filling of the d bands in structures of high symmetry, is the main topic of their discussion.

The small transition metal clusters are models of catalytic active sites, which are usually associated with surface defects, characterized by a local electron deficiency. A Mulliken population analysis (table 2) shows a negative charge (-0.175 au) largely concentrated on the atom in the center, counterbalanced

by a small positive charge (0.015 each atom) distributed among the peripheral atoms. Previous calculations on the interaction of CO with Rh clusters [24] have demonstrated larger activity towards CO adsorption on electron deficient sites, characteristics of the *surface atoms*, in the precrystalline structures. The study of the electronic characteristics imply, thence, practical importance, and can only be analyzed after a complete study of the structure of minimun energy.

3.4- On the stability of the highly symmetric structures -

The electronic degeneracy in a molecule forces departures from the symmetry on which the degeneracy was evaluated [51,52]. Therefore, for non-linear molecules, a nuclear arrangement that will lead to electronic degeneracies will automatically have at least one non-totally symmetric vibrational coordinate that will split the degenerate state and destroy the symmetry. When degeneracy occurs, only those systems where the number of electrons either completely fill or half-fill sets of degenerate one-electron levels will not Jahn-Teller distort. As this is not the case of either Pd_{13} or Pd_4 structures, the nature of the distortion should be evaluated.

The large stability of the I_h and T_d structures for the 13 and 4 atom clusters respectively, allowed us to obtain these structures through configuration averaging. This, of course, is an intermediate stage we examine to make comparisons with the work of others, and one which will allow us to examine the Jahn-Teller distorsions in some detail. Of interest is that we were unable by any means to successfully obtain the full I_h structure for Rh_{13}. Rather, a *near* C_{5v} symmetry is achieved from both I_h and O_h starting geometries [25]. We have not been able to analyze quantitatively the steps and the normal modes involved in the distortion of the Rh_{13} molecule from I_h to C_{5v}, although we could for Rh_{13}^+ [25].

In order to analyze this effect for Pd, and to learn about distortions that may lower the energy through the splitting of the degenerate orbitals, different initial geometries have been

compared, which are related through a normal mode to the higher symmetry ones.

a- Icosahedral Pd_{13} clusters.

According to the electronic distribution depicted in Fig 3, the Jahn-Teller theorem requires a splitting of the $(t_{2g})^4 = {}^3T_{2g} + {}^1H_g + {}^1A_g$ degeneracy, leading to orbitals of e_{2g} and a_{2g} symmetry in D_{5d}. Correspondingly, the ${}^3T_{2g}$ state reduces to ${}^3E_{2g}$ and ${}^3A_{2g}$, the ${}^1H_g$ state to states of ${}^1A_{1g}$, ${}^1E_{1g}$ and ${}^1E_{2g}$ symmetry and ${}^1A_g$ becomes ${}^1A_{1g}$, see Fig. 4. The relative positions of the e_{2g} and a_{2g} orbitals in energy depend on the final geometry. The simpler distortions that can be idealized imply an axial elongation along the principal axis in D_{5d} symmetry (z axis, Fig 2) or an axial compression along the same axis, to give *prolate or oblate ellipsoids* respectively, from an initial *spheroid* I_h structure. Depending on the characteristics of the distortion, the e_{2g} orbital will be above or below the a_{2g} for the elongated or compressed geometries respectively.

In the case of Pd_{13}, the prolate or oblate distorted starting structures returns to the perfect I_h after optimizing the geometry. Starting structures resulting from prolate or oblate distortions along a 3 fold axis in D_{3d} symmetry, or a 2-fold axis in D_{2h} symmetry, also lead to the perfect I_h.
After several trials, a related structure was found, with lower energy than the initial ${}^3T_{2g}$. It is the result of an elongation of the Pd_{13} I_h molecule along the principal axis in D_{5d} symmetry, coupled to a compression along the same axis that shortens the distance between oppossite pentagons (Fig. 5). This corresponds to an h_g mode in I_h symmetry.

The molecular orbital distribution in the D_{5d} structure shows the e_{2g} orbital below the a_{2g} (Fig.3). The lowest energy corresponds to a singlet (${}^1A_{1g}$), followed by a triplet (${}^3E_{2g}$), which lies 0.16 eV above. The next states are a triplet and a singlet which lie 0.31 and 0.49 eV, respectively, higher in energy than the GS, see Fig 5.

The distortion of the geometry can be described as a first order Jahn-Teller effect from the ${}^3T_{2g}$, in I_h symmetry, to the

$^3E_{2g}$ in D_{5d}, through an hg mode, with an energy decrease of 0.9 Kcal. Further decay to the singlet $^1A_{1g}$ decreases the energy through spin pairing to give a closed- shell structure (Fig. 5). The GS of the Jahn-Teller distorted structure is 4.68 Kcal below the *spherical* $^3T_{2g}$. An alternative conceptual description may involve the lowest singlets in I_h and D_{5d} symmetries. An initial activation from the triplet to the singlet implies, however, an energy barrier of 0.21 eV. We stress *conceptual* as the Jahn-Teller effect is a theoretical construction to describe distortions, not a physical one. One does not observe I_h distorting to D_{5d}, one simply observes D_{5d}.

A Mulliken population analysis of the D_{5d} GS structure shows that a negative charge (-0.154 au) is still located on the atom in the center, while the positive charge is now more concentrated on the apical atoms (+0.149 au on each). This allows one to infer a larger catalytic activity of these centers.

Although the highly symmetric structures are characterized by a non-zero magnetic moment, the stabilization through a Jahn-Teller distortion, followed by spin pairing, results in a prediction of diamagnetic Pd_{13} clusters.

The consecutive *geometric distortion- followed by electron pairing* shows the importance of this interplay: the geometry of the final (distorted) state, which is a consequence of the electronic distribution in the higher symmetry one, leads to spin quenching.

Providing that there is not a large change in the geometry and that the molecular orbital distribution is nearly kept, the positively charged Pd_{13}^+ structure would give a perfect icosahedron which would not distort, due to the equivalent filling of the degenerate t_{2g} HOMO orbitals. The optimization of the geometry gives a perfect icosahedron (Fig 2), with an interatomic distance of 2.63 A and a molecular orbital distribution similar to that in the neutral but for the t_{2g} - h_g inversion and the larger HOMO-LUMO gap (Fig 6). The GS is a quartet ^4A_g, followed by a doublet ^2H_g, which is 0.22 eV higher in energy.

Pd_{13}^{+} clusters would be predicted to have non- zero magnetic moments.

b- Tetrahedral Pd_4 clusters.

The tetrahedral Pd_4 clusters are predicted to have $^3T_2$ symmetry, and they also suffer a first order Jahn-Teller distortion.

After examining several structures, we find that the most stable structure, depicted in Fig 7, corresponds to a $^3A_2$ in C_{2v} symmetry, and is the result of a Jahn-Teller distortion of the $^3T_2$ in T_d symmetry through an e mode. There is no extra stabilization through spin pairing. The GS in C_{2v} is a non-degenerate triplet, with the lowest singlet, $^1A_2$, 0.38 eV higher in energy. The energy associated to the distortion is 0.08 eV (1.84 Kcal).

The Pd_4 clusters are, thence, paramagnetic.

4- CONCLUSIONS -

In agreement with previous results on Rh_{13} and Rh_4 clusters, we have found that Icosahedral and Tetrahedral geometries are, respectively, the most stable ones for the higher symmetric structures. Both Ih and Td structures are characterized by a large concentration of triangular faces, which are the minimun part of an fcc(111) structure, associated with the larger packing density and the lower total energy for this crystalline habit. This is accepted as a valid explanation of the larger stability of these geometries for the cluster sizes analyzed. The final geometries are, however, largely determined by Jahn-Teller distortions, that we predict lower the I_h and T_d geometries to D_{5d} and C_{2v} structures, respectively.

A small energy difference between the symmetrical and the distorted structure may determine the spontaneous evolution to the latter. This effect, previously found in Rh_{13} clusters, does not characterize either Pd_{13} or Pd_4 clusters, and the different steps involved in the distortion can be analyzed. This analysis, discussed in this paper, shows the close relation and mutual

dependence between the electronic structure and the geometry of the small structures.

The electronic configuration of the final structure, which we found determined by a Jahn-Teller distortions in both Pd_4 and Pd_{13} defines the magnetic moment of the tiny particles. While we calculate that paramagnetism characterizes Pd_4 clusters, the most stable Pd_{13} structures have zero magnetic moment. Recent density functional calculations [50] have found a non-zero magnetic moment ($-2\mu_B$), based on a most stable I_h symmetry. This is in agreement with our results for this structure. But our final structure is a distorted I_h cluster of D_{5d} geometry and has a zero magnetic moment. This agrees with the zero magnetic moment experimentally found [53].

- ACKNOWLEDGEMENTS -

This work was supported in part through grants from the Consejo Nacional de Investigaciones Científicas y Técnicas (CONICET) and Fundación Antorchas (República Argentina) and the Office of Naval Research (USA).

- REFERENCES -

1- V. Bonacic-Koutecky, P. Fantucci and J. Koutecky, Chem. Rev. (1991), **91**, 1035.

2- J. C. Phillips, Phys. Rev.B (1993), **47**, 14132.

3- J. Demuynck, M. Rohmer, A. Strich and A. Veillard, J. Chem. Phys. (1981), **75**, 3443.

4- J. L. Martins, J. Buttet and R. Car, Phys. Rev.B (1985), **31**, 1804.

5- G. Pacchioni and J. Koutecky, J. Chem. Phys. (1984), **81**, 3588.

6- K. Raghavan, M. S. Stave and A. DePristo, J. Chem. Phys. (1989), **91**, 1904.

7- O. B. Christensen, K. W. Jacobsen, J. K. Norskov and M. Manninen, Phys. Rev. Lett. (1991), **66**, 2219.

8- M. Harbola, Proc. Natl. Acad. Sci USA (1992), **89**, 1036.

9- B. K. Rao, S. N. Khanna and P. Jena, Ultramicroscopy (1986), **20**, 51.

10- H. P. Cheng, R. S. Berry and R. L. Whetten, Phys. Rev. B (1991), **43**, 10647.

11- S. Valkealahti and M. Manninen, Phys. Rev. B (1992), **45**, 9459.

12- K. K. Das and K. Balasubramanian, J. Chem. Phys. (1990), **93**, 325.

13- F. Illas, J. Rubio and J. Canellas, J. Chem. Phys. (1990), **93**, 2603.

14- C. Yannouleas, J. M. Pacheco and R. A. Broglia, Phys. Rev. B (1990), **41**, 6088.

15- a- B. J. Winter, T. D. Klots, E. K. Parks and S. J. Riley, Z. Phys. D- Atoms, Molecules and Clusters (1991), **19**, 375. b- B. J. Winter, E. K. Parks and S. J. Riley, J. Chem. Phys. (1991), **94**, 8618.

16- J. Jellinek and Z. B. Guvenc, Z. Phys. D- Atoms, Molecules and Clusters (1991), **19**, 371.

17- B. G. Ershov, E. Janata and A. Henglein, J. Phys. Chem. (1993), **97**, 339.

18- D. F. Rieck, J. A. Gavney, R. L. Norman, R. K. Hayashi and L. F. Dahl, J. Am. Chem. Soc. (1992), **114**, 10369.

19- J. P. Zebrowsky, R. K. Hayashi and L. F. Dahl, J. Am. Chem. Soc. (1993), **115**, 1142.

20- T. D. Klots, B. J. Winter, E. K. Parks and S. J. Riley, J. Chem. Phys. (1990), **92**, 2210.

21- E. K. Parks, B. J. Winter, T. D. Klots and S. J. Riley, J. Chem. Phys. (1991), **94**, 1882.

22- *Metal Clusters*, M. Moskovits ed. John Wiley & Sons. Wiley Interscience Publication, 1986.

23- G. L. Estiú and M. C. Zerner, Int. J. Quantum Chem. (1992), **26**, 587.

24- G. L. Estiú and M. C. Zerner, Int. J. Quantum Chem., in press.

25- G. L. Estiú and M. C. Zerner, J. Phys. Chem., in press.

26- K. Sattler, J. Muhlbach and E. Recknagel, Phys. Rev. Lett. (1980), **45**, 821.

27- J. G. Fripiat, K. T. Chow, M. Boudart, J. R. Diamond and K. H. Johnson, J. Mol. Catal. (1975), **1**, 59.

28- A. Renou and M. Gillet, Surf. Sci. (1981), **106**, 27.

29- B. K. Teo, H. Zhang, Proc. Natl. Acad. Sci USA (1991), **88**, 5067.

30- C. E. Briant, B.R. Theobald, J. W. White, L. K. Bell, D. M. P. Mingos and A. J. Welch, J. Chem. Soc., Chem. Commun. **1981**, 201.

31- C. E. Briant, K. P. Hall, A. C. Wheeler and D. M. P. Mingos and A. J. Welch, J. Chem. Soc., Chem. Commun. **1984**, 248.

32- R. B. King, Inorg. Chim. Acta, (1986), **116**, 109.

33- B. T. Heaton, L. Strona, R. D. Pergola, J. L. Vidal and R. C. Schoening., J. Chem. Soc., Dalton Trans. **1983**, 1941.

34- M. C. Zerner, ZINDO Package. Quantum Theory Project. Williamson Hall. University of Florida.

35- W. D. Edwards and M. C. Zerner, Theoret. Chim. Acta, (1987), **72**, 347.

36- a) J. D. Head and M. C. Zerner, Chem.Phys. Letters (1985), **122**, 264. b) J. D. Head and M. C. Zerner, Chem. Phys. Letters (1986), **131**, 359.

37- J. D. Head, B. Weiner and M. C. Zerner, Int. J. Quantum Chem. (1988), **33**, 177.

38- M. C. Zerner, Int. J. Quantum Chem. (1989), **35**, 567.

39- R. Pauncz, *Spin Eigenfunctions* (Plenum Press, New York, 1979).

40- W. P. Anderson, T. R. Cundari and M. C. Zerner, Int. J. Quantum Chem. (1991), **34**, 31.

41- M.C. Zerner in *Reviews in Computational Chemistry*. Vol.2. K. B. Lipkowitz and B. Boyd eds. VCH Publishers. New York, 1990.

42- J. P. Stewart in *Reviews in Computational Chemistry*. Vol.1. K. B. Lipkowitz and B. Boyd eds. VCH Publishers. New York, 1990.

43- A. Goursot, I. Papai and D. R. Salahub, J. Am. Chem. Soc. (1992), **114**, 6452.

44- I. Papai, A. Goursot, St-Amant and D. R. Salahub, Theor. Chim. Acta. To appear.

45- K. Balasubramanian, J. Chem. Phys. (1988), **89**, 6310.

46- K. Balasubramanian, J. Chem. Phys. (1989), **91**, 307.

47- K. Balasubramanian and D. Liao, J. Phys. Chem. (1989), **93**, 3989.

48- K. Balasubramanian, J. Phys. Chem. (1989), **93**, 6585.

49- D. R. Lide, *CRC Handbook of Chemistry and Physics* (CRC Press, Boca Ratón, FL, 1990-91).

50- B. V. Reedy, S. N. Khanna and B. I. Dunlap, Phys. Rev. Lett. (1993), **70**, 3323.

51- H. A. Jahn and E. Teller, Proc. R. Soc. London Ser. A (1937), **161**, 220.

52- G. Herzberg, *Molecular spectra and Molecular Structure. III. Electronic Spectra and Electronic Structure of Poliatomic Molecules*. Van Nostrand Reinhold Company, NY, 1966.

53- D. C. Douglas, J. P. Bucher and L. A. Bloomfield, Phys. Rev. B (1992), **45**, 6341.

- FIGURE CAPTIONS -

- Figure 1 - The frontier molecular orbitals obtained for Pd_4 in T_d symmetry and the distorted molecule in C_{2v} symmetry. The distortion that relates both structures is indicated. Energies are in Hartrees.
- Figure 2 - Most stable Pd_{13} structure as result from a full geometry optimization procedure, starting from an Ih initial structure.The symmetry is kept when 4 electrons are averaged in 3 orbitals in the CAHF calculations. More details are given in the text.
- Figure 3 - The frontier molecular orbitals obtained for Pd_{13} in I_h symmetry and the distorted molecule in D_{5d} symmetry. The distortion that relates both structures is indicated. Energies are in Hartrees.
- Figure 4 - Electronic states associated to the I_h -> D_{5d} Jahn-Teller distortion of the Pd_{13} structure.
- Figure 5 - Distortion of the Pd_{13} molecule, in I_h symmetry, to the most stable one in D_{5d} symmetry. Geometrical parameters are indicated.
- Figure 6 - The frontier molecular orbitals obtained for Pd_{13}^+ in I_h symmetry, from CAHF calculations with 3 electrons in 3 orbitals. Because of the half filling of degenerate orbitals, the molecule does not Jahn-Teller distort. The symmetry of the resulting state is ^4A_g.
- Figure 7 - Distortion of the Pd_4 molecule, in T_d symmetry, to the most satble one in C_{2v} symmetry. Geometric parameters are indicated.

M	1	3	5	7	r[A]	M.P.
RHF	-118.061 $^1T_2$	-118.063 $^3T_2$	-118.021 $^5T_1$	-117.930 $^7T_2$	2.683	$5s^{0.31}5p^{0.}{}^{22}4d^{9.47}$
4/3	-118.082 $^1A_1$	-118.097 $^3T_2$	-118.070 $^5T_1$	-118.052 $^7T_2$	2.390	$5s^{0.52}5p^{0.}{}^{26}4d^{9.21}$
4/6	-117.955 $^1A_1$	-117.995 $^3T_2$	-117.985 $^5T_1$	-117.934 $^7T_2$	2.321	$5s^{0.52}5p^{0.}{}^{24}4d^{9.23}$
6/9	-117.857 $^1A_1$	-117.871, $^3T_2$	-117.862 $^5T_1$	-117.812 $^7T_2$	2.286	$5s^{0.46}5p^{0.}{}^{25}4d^{9.26}$
bulk	-118.075 $^1A_1$	-118.093 $^3T_2$	-118.020 $^5T_1$	-118.001 $^7T_2$	2.750	$5s^{0.53}5p^{0.}{}^{14}4d^{9.32}$

Table 1- Absolute values of the total energies [Hartrees] calculated for Pd_4 tetrahedral structures after MRCIS calculations. Electronic states are also indicated. Different M are compared for the different geometries that result from RHF (1st row) or CAHF calculations with different number of open shells included in the average. 4/3, 4/6 and 6/9 stands for 4 e^- in 3 orbitals, 4 e^- in 6 orbitals, and 6 e^- in 9 orbitals, respectively.

In the last row, calculations for the bulk interatomic distance are reported. The Mulliken populations (M.P.) given are for the triplet, see text.

	Ih		Oh		D3h	
M	Energy	State	Energy	State	Energy	State
1	-384.504	^1H_g	-384.445	^1A_g	-384.447	$^1A_1"$
3	-384.512	$^3T_{2g}$	-384.435	$^3T_{2g}$	-384.445	$^3A_1"$
5	-384.487	^5T_u	-384.406	$^5T_{1u}$	-384.410	$^5A_1'$
M.P.	$5s^{0.40}$ $5p^{0.78}$ $4d^{9.10}$		$5s^{0.54}$ $5p^{0.75}$ $4d^{9.15}$		$5s^{0.54}$ $5p^{0.74}$ $4d^{9.22}$	
r[A]	Fig. 1		2.54		2.55	

Table 2- The total valence energies [hartrees] calculated for Pd_{13} structures after MRCIS calculations. Electronic states are also indicated. Different M are compared for the geometries associated with the I_h, O_h and D_{3h} symmetries. Details on the calculations are given in the text. The Mulliken populations (M.P.) are reported for the central atom and correspond to the most stable M for each geometry.

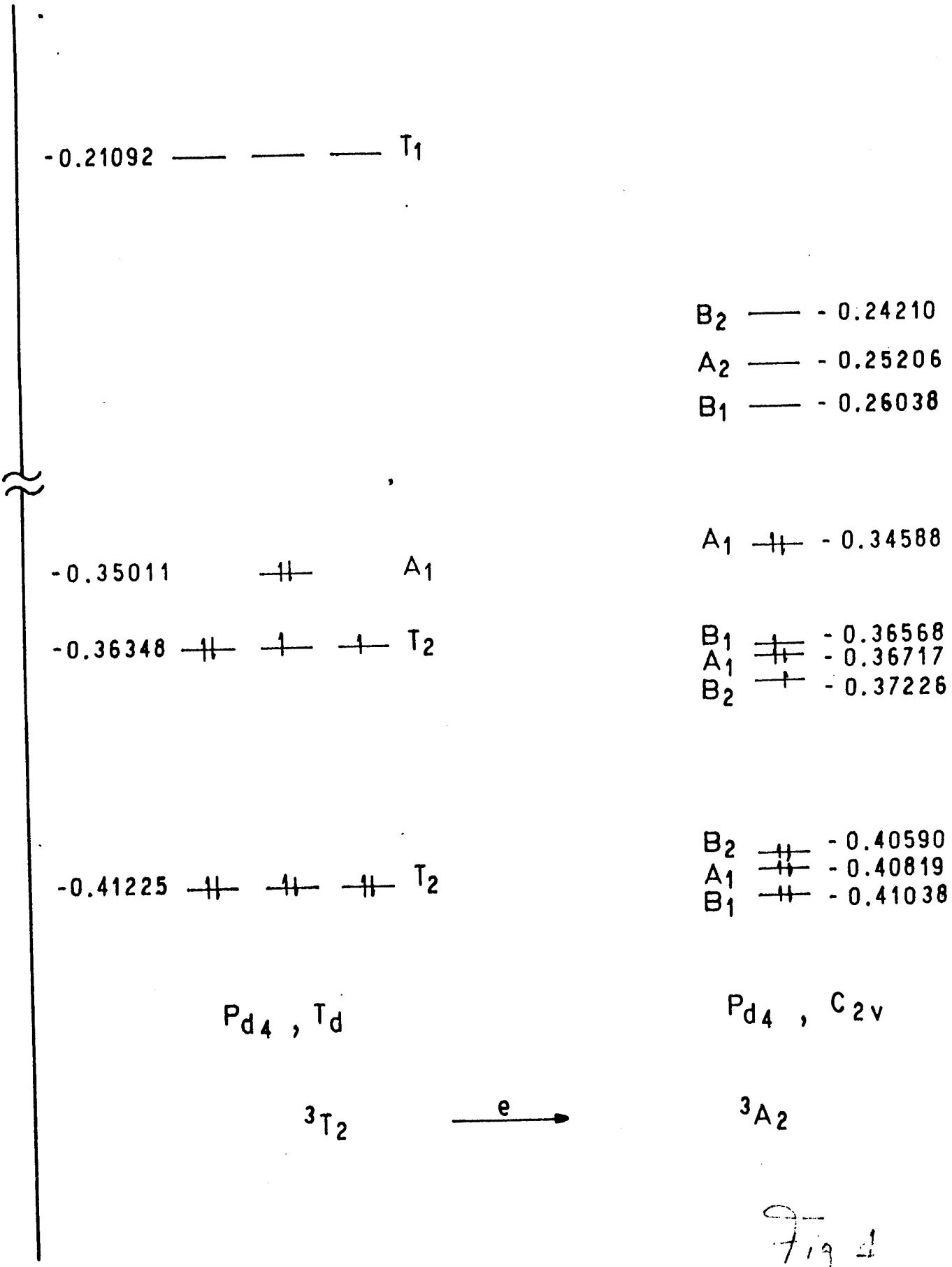
-0.21092 T1
B2 - 0.24210
A2 - 0.25206
B1 - 0.26038
A1 - 0.34588
-0.35011 A1
-0.36348 T2
B1 - 0.36568
A1 - 0.36717
B2 - 0.37226
B2 - 0.40590
A1 - 0.40819
B1 - 0.41038
-0.41225 T2
Pd4 , Td
Pd4 , C2v
3T2
e
3A2

Fig 4

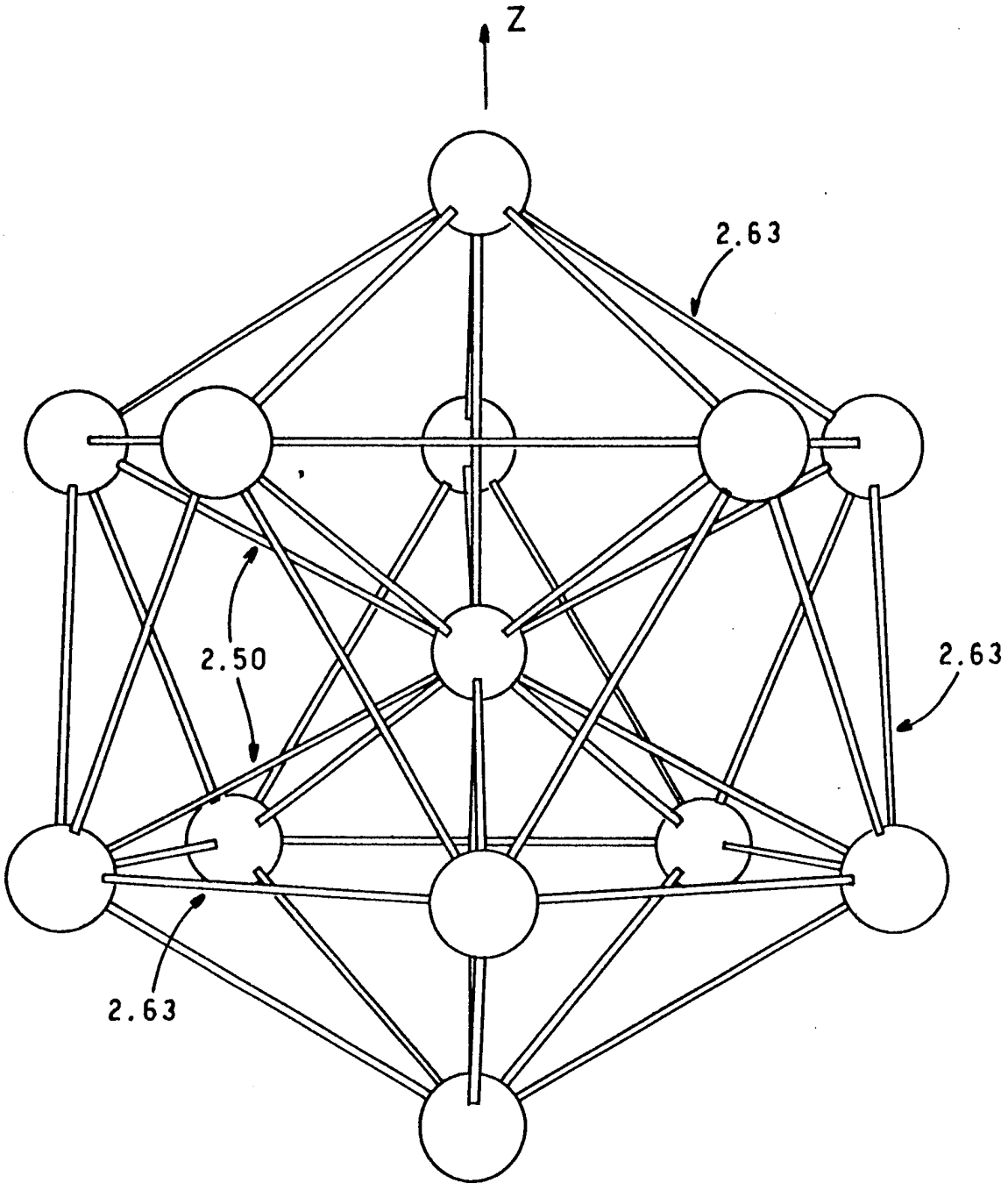

Fig 2

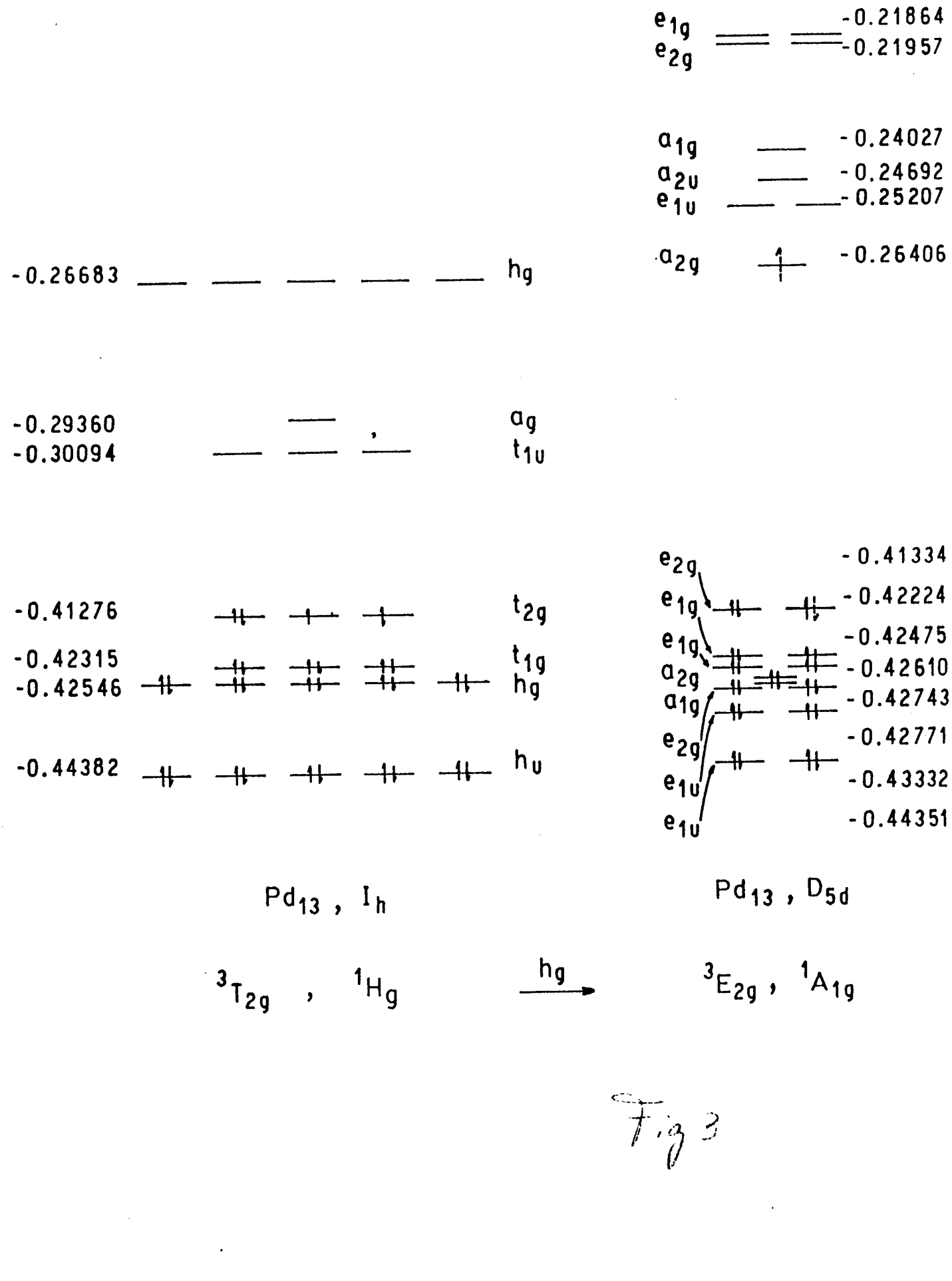
e1g -0.21864
e2g -0.21957
a1g -0.24027
a2u -0.24692
e1u -0.25207
a2g -0.26406
-0.26683 hg
-0.29360 ag
-0.30094 t1u
-0.41276 t2g
-0.42315 t1g
-0.42546 hg
-0.44382 hu
e2g -0.41334
e1g -0.42224
e1g -0.42475
a2g -0.42610
a1g -0.42743
e2g -0.42771
e1u -0.43332
e1u -0.44351
Pd13 , Ih
3T2g , 1Hg
hg
Pd13 , D5d
3E2g , 1A1g

Fig 3

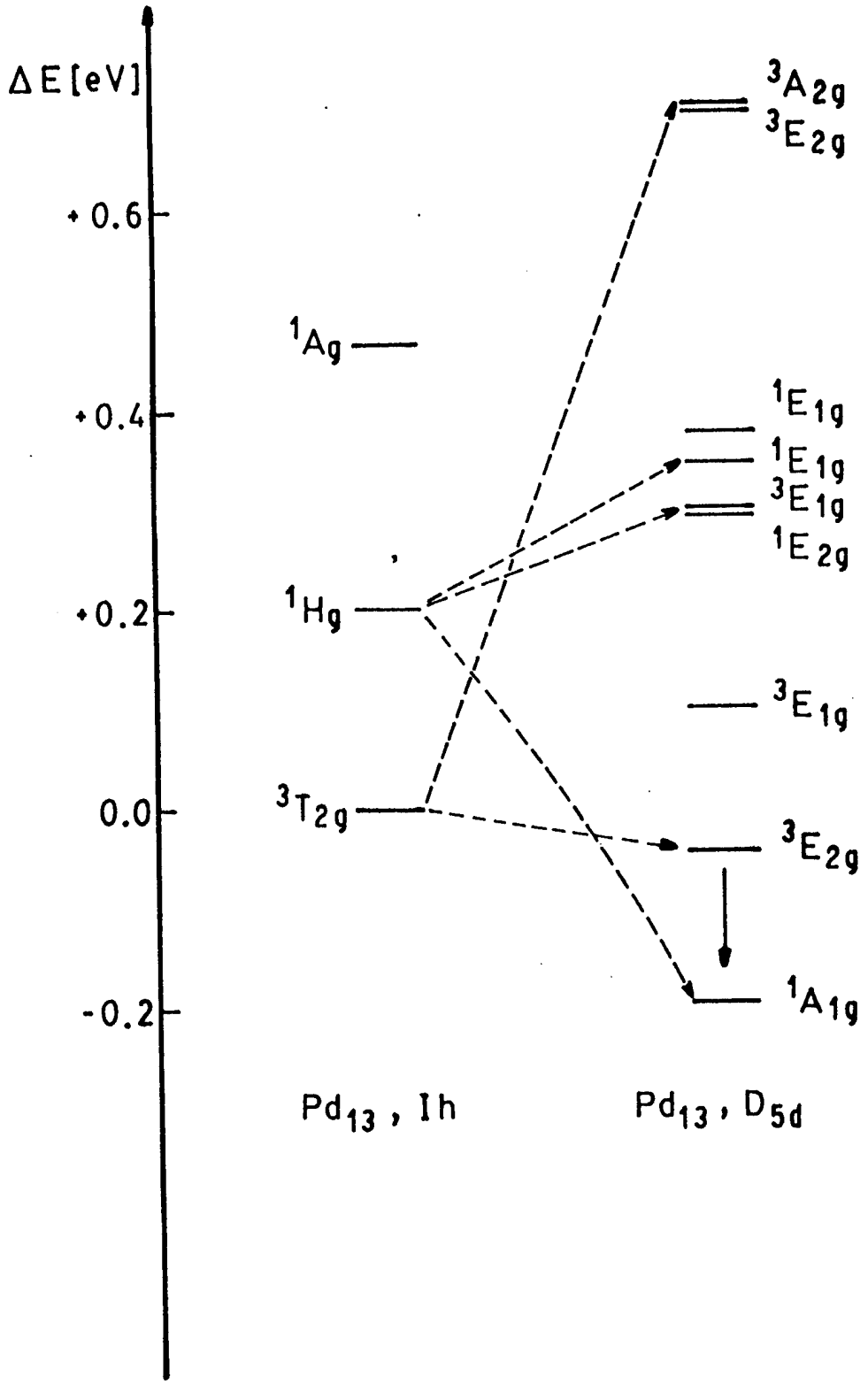
ΔE [eV]
+0.6
+0.4
+0.2
0.0
-0.2
$^3A_{2g}$
$^3E_{2g}$
^1A_g
$^1E_{1g}$
$^1E_{1g}$
$^3E_{1g}$
$^1E_{2g}$
^1H_g
$^3E_{1g}$
$^3T_{2g}$
$^3E_{2g}$
$^1A_{1g}$
Pd_{13}, Ih
Pd_{13}, D_{5d}

Fig 4

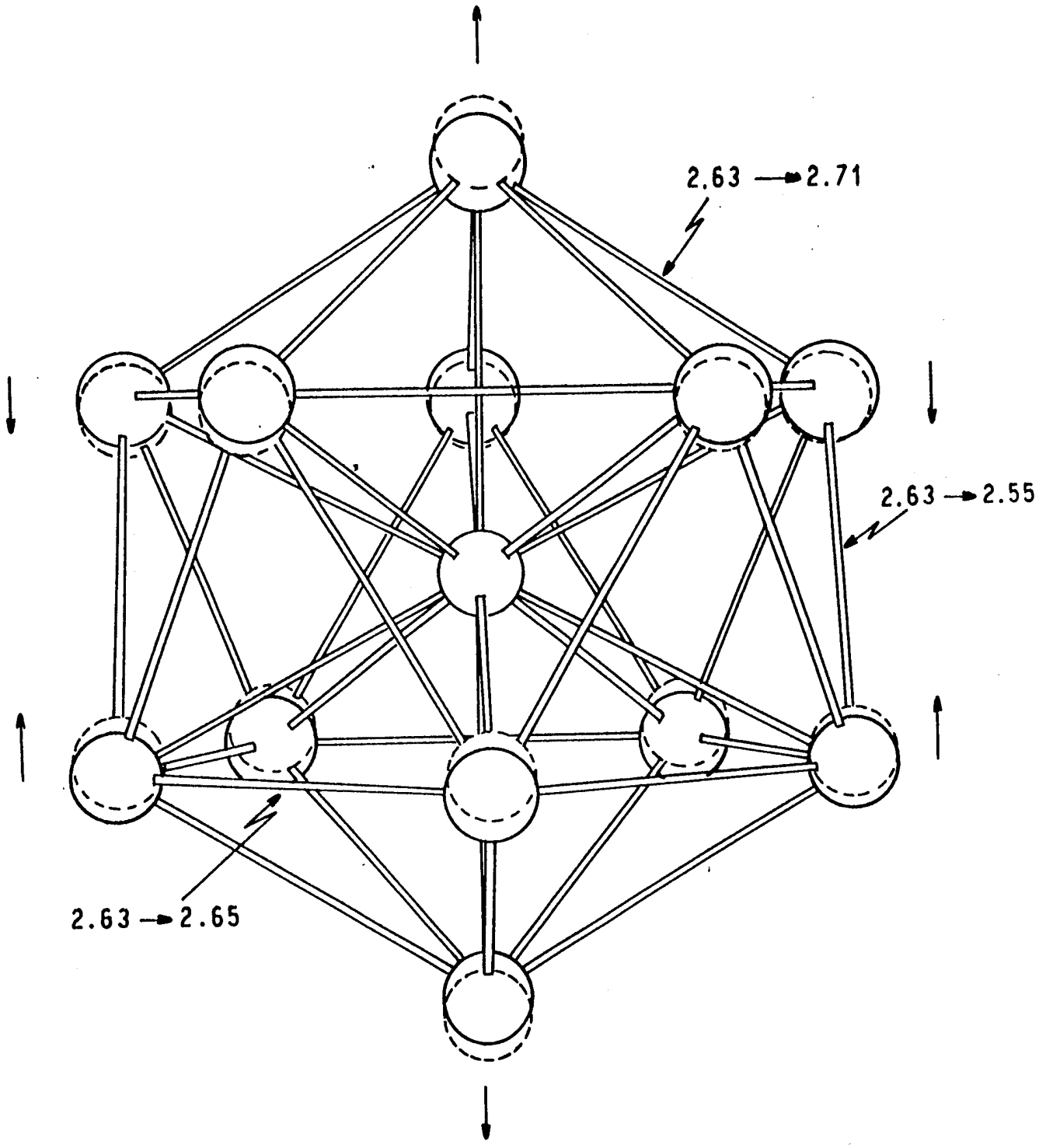

$I_h \longrightarrow D_{5d}$

Fig 5

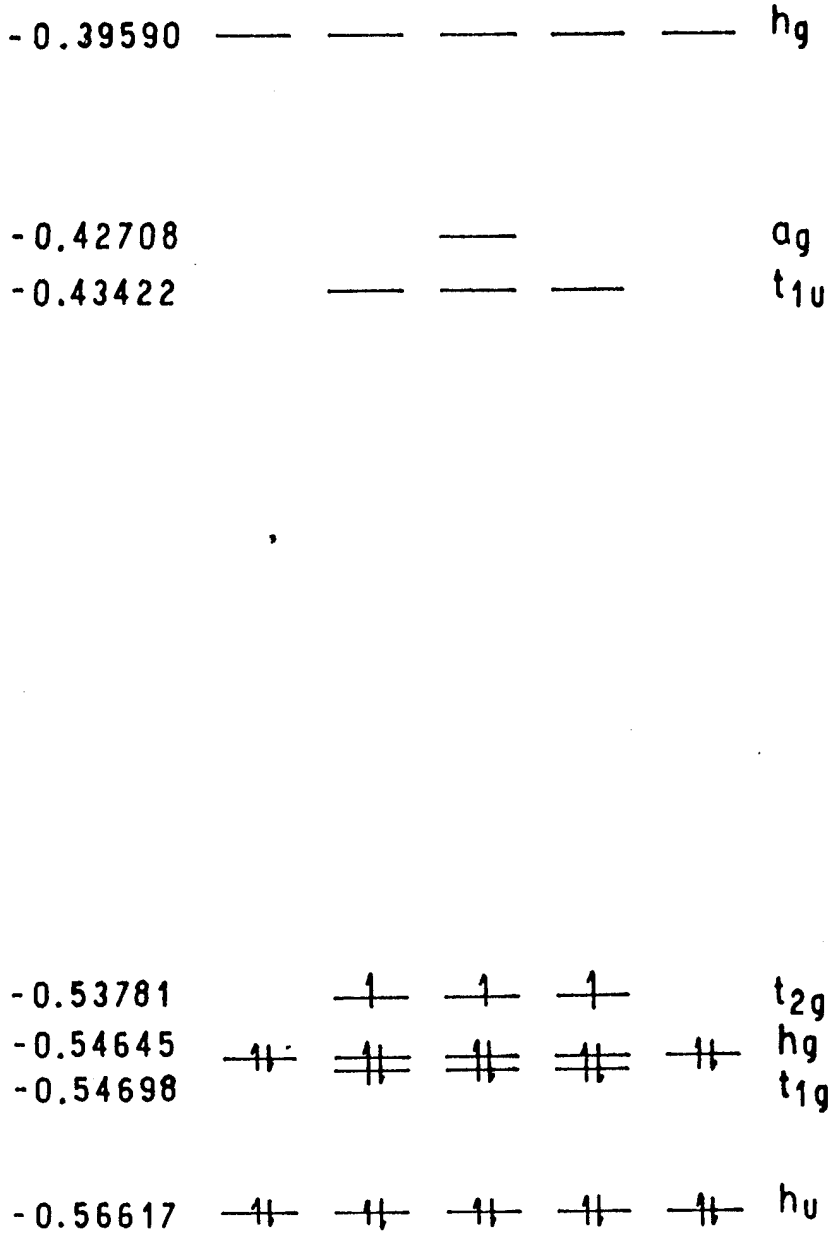
-0.39590
hg
-0.42708
ag
-0.43422
t1u
-0.53781
t2g
-0.54645
hg
-0.54698
t1g
-0.56617
hu

Pd_{13}^{+} , Ih

Fig 6

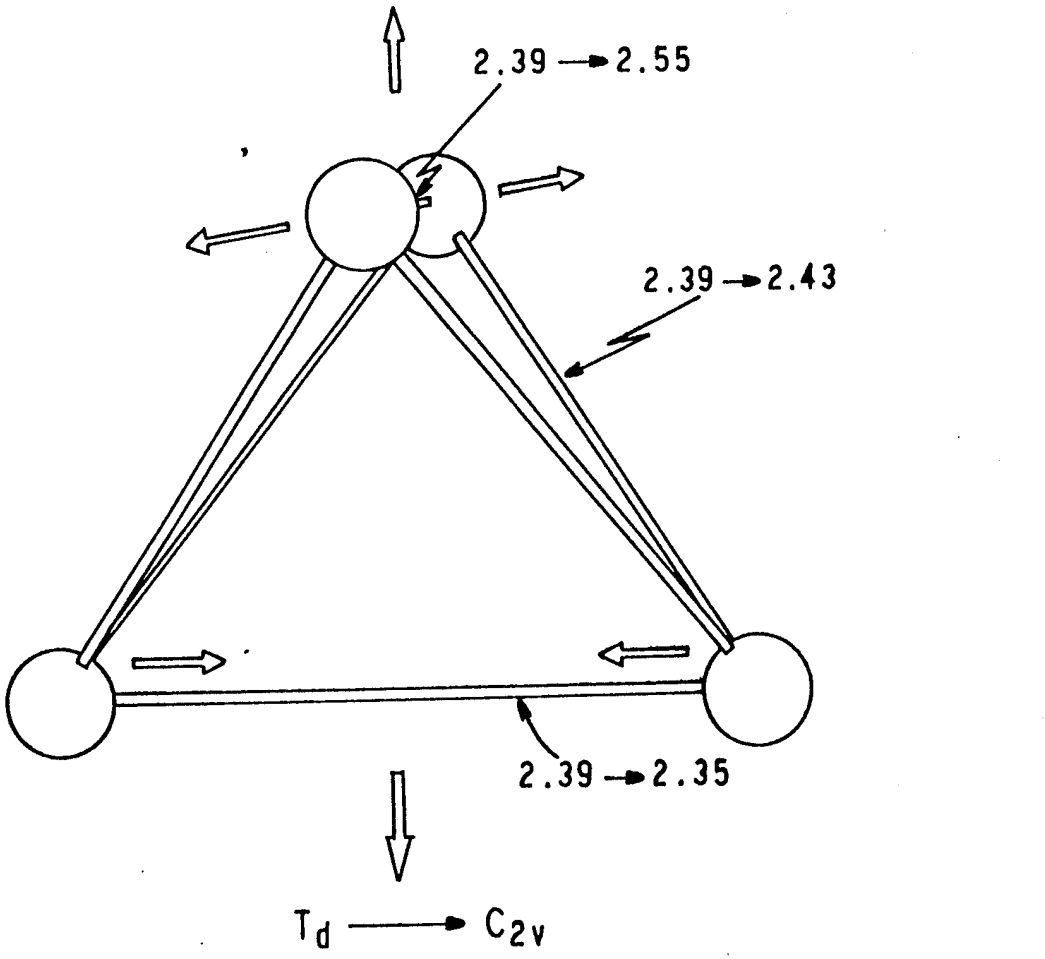

Fig 7